Wang *et al. Chem Synth* 2024;4:24
DOI: 10.20517/cs.2024.04

Chemical Synthesis

Research Article

Open Access

Highly selective production of renewable methyl acrylate via aldol condensation over Cu modified nitrogen-containing Beta zeolites

Mei Wang, Lulu Xu, Weiping Zhang*

State Key Laboratory of Fine Chemicals, School of Chemical Engineering, Dalian University of Technology, Dalian 116024, Liaoning, China.

***Correspondence to:** Prof. Weiping Zhang, State Key Laboratory of Fine Chemicals, School of Chemical Engineering, Dalian University of Technology, No. 2 Linggong Road, Dalian 116024, Liaoning, China. E-mail: wpzhang@dlut.edu.cn

How to cite this article: Wang M, Xu L, Zhang W. Highly selective production of renewable methyl acrylate via aldol condensation over Cu modified nitrogen-containing Beta zeolites. *Chem Synth* 2024;4:24. https://dx.doi.org/10.20517/cs.2024.04

Received: 12 Jan 2024 **First Decision:** 28 Mar 2024 **Revised:** 28 Mar 2024 **Accepted:** 2 Apr 2024 **Published:** 18 Apr 2024

Academic Editor: Jun Xu **Copy Editor:** Dong-Li Li **Production Editor:** Dong-Li Li

Abstract

Highly selective synthesis of renewable methyl acrylate from bio-sourced formaldehyde and methyl acetate through one-step aldol condensation was successfully realized on Cu-modified nitrogen-containing Beta (NBeta) catalysts. Silicon-29 magic angle spinning nuclear magnetic resonance (^{29}Si MAS NMR), Fourier transform infrared spectroscopy (FT-IR), temperature-programmed desorption of ammonia, temperature-programmed desorption of carbon dioxide, and element analysis indicate that nitridation weakens the acid strength, reduces the number of acidic sites and introduces basic sites through the formation of Si–N bond on Beta zeolites, thereby promoting methyl acrylate selectivity and reducing the coke formation. Adding Cu into NBeta further finely tunes the basicity and acidity balance and thus inhibits the by-product acetone. High methyl acrylate selectivity of 95% and formaldehyde conversion of 99% were achieved over Cu/NBeta catalyst under optimized conditions. The coke content decreases remarkably from 28% on H-form Beta (HBeta) zeolites to 17% on NBeta zeolites doped with Cu due to its appropriate basicity/acidity. Cu/NBeta has good regeneration capability, and the weakening of Si-N species may account for the decline of catalytic performance after successive regeneration. The catalytic performance was restored when the regenerated catalyst was nitridated again.

Keywords: Nitrogen-containing Beta zeolites, aldol condensation, renewable methyl acrylate, basicity, acidity

INTRODUCTION

As important intermediates in organic synthesis, acrylic acid and its derivatives, such as methyl acrylate, are widely used in producing adhesives, synthetic resins, and paint and coating additives[1,2]. Acrylic acid can be obtained through the two-step oxidation of propylene, of which the first step is propylene oxidation to acrolein, then further oxidation to acrylic acid[3], and esterification to methyl acrylate. This process is long and complex, and there is a risk of excessive oxidation of propylene and the required products. In addition, this route depends on the fossil resources and is not environmentally benign and sustainable. Therefore, it is essential to develop a new alternative. In recent years, the one-step preparation of methyl acrylate from methyl acetate and formaldehyde through the aldol condensation has attracted extensive attention[4-6]. This is a promising and even renewable pathway for producing methyl acrylate because both the feedstocks, formaldehyde and methyl acetate, can be derived from bio-based methanol[7].

At present, aldol condensation reactions are mainly carried out on solid catalysts, including acidic[4,8,9], basic[5,10], and acid-base bifunctional catalysts[11-13]. Solid acidic catalysts mainly include phosphates[8] and zeolites[9,14]. Khalameida *et al.* reported titanium phosphates for aldol condensation of acetic acid and formaldehyde with an acrylic acid selectivity of 80%[8]. Ma *et al.* used HZSM-35 and Cs/ZSM-35 zeolites to catalyze the aldol condensation[6,9]. They believed that the medium and weak strong acids in the catalyst benefit this reaction. Although solid acidic catalysts have fairly good catalytic performance, the selectivity of methyl acrylate is relatively low due to many side reactions caused by the strong acidic sites. Solid basic catalysts are mainly supported alkali metal/alkaline earth metal catalysts[5,10,15]. He *et al.* loaded Li, Na, K, Rb, and Cs on SBA-15 to catalyze the reaction of methyl acetate and formaldehyde to synthesize methyl acrylate[16]. They found that Cs/SBA-15 had the best reaction performance, and the selectivity of methyl acrylate was 91%[5]. Yan *et al.* also obtained the similar results on Cs/SBA-15 with methyl acrylate selectivity of 95%, but the conversion of methyl acetate was as low as 48%[17]. Although supported basic catalysts have high selectivity for methyl acrylate, they are usually unstable, prone to deactivation and difficult to regenerate. The acid-base bifunctional catalysts with balanced acidic and basic properties show good catalytic performance in aldol reaction owning to the acid-base synergistic effect[18,19]. Formaldehyde is protonated to form C^+ cation on the acidic site, and methyl acetate is activated to remove α-H to form α-C^- anion on the basic site. Then, the addition of the C^+ cation to the α-C^- anion forms an unstable intermediate aldol, and a molecule of water is removed on an acidic site to form methyl acrylate[12]. Bao *et al.* reported a bifunctional Ba-La/Al_2O_3 catalyst, the conversion of methyl acetate was ~40%, and the selectivity of methyl acrylate was ~94%[20]. Guo *et al.* demonstrated that the vanadium phosphorus (VP) oxide catalyst with a P/V atomic ratio of 1.2 exhibited the best activity due to the higher fraction of $VOPO_4$ entity and $(VO)_2P_2O_7$ phase with balanced acidity and basicity[21]. Zhao *et al.* reported that γ-Al_2O_3 loaded VP oxide (VPO) exhibited a conversion of 42% for formaldehyde and a selectivity of 92% for methyl acrylate[22]. VPO supported on SBA-15 and HZSM-5 also showed good performance to prepare methyl acrylate[23]. However, VPO catalyst systems are relatively complex, and many factors such as phase composition, V^{4+}/V^{5+} ratio, support and promoter[24,25] affect their activity. Therefore, it is necessary to develop the simple and efficient acid-base bifunctional catalysts for aldol reaction and the relationship between acidity/basicity and activity needs to be further understood. High-temperature nitridation of zeolites in ammonia results in both acidic and basic sites on the surface[26-28], which has been applied in some acid-base catalytic reactions[29-31]. However, the preparation of methyl acrylate by aldol condensation catalyzed by nitrogen-containing zeolites has not been well studied.

In this paper, we prepared the nitrogen-containing Beta (NBeta) from H-form Beta (HBeta) zeolites through nitridation in ammonia at high temperatures, and their catalytic performance of the aldol condensation to prepare methyl acrylate was compared in detail. Addition of Cu into NBeta was employed

to tune the acidity and basicity and further improved the reaction performance. The reactivity correlation with the structure and acid-base properties was revealed by X-ray diffraction (XRD), N_2 adsorption, elemental analysis, silicon-29 magic angle spinning nuclear magnetic resonance (^{29}Si MAS NMR), Fourier transform infrared spectroscopy (FT-IR), temperature-programmed desorption (TPD) of ammonia (NH_3-TPD), and TPD of carbon dioxide (CO_2-TPD). The regeneration capability and deactivation mechanism of the spent catalyst was also investigated.

EXPERIMENTAL

Catalyst preparation

NH_4Beta zeolites (Si/Al = 19, Zeolyst) were calcinated at 550 °C in a muffle furnace to obtain HBeta. The nitridation of HBeta zeolites was performed in an NH_3 flow at high temperatures. The samples obtained were denoted as NB-*p*, where *p* represents the nitridation temperature, ammonia flow rate, or nitridation time.

The supported Cu/NBeta catalysts with different Cu contents were prepared by impregnating NBeta zeolites with desired amount of $Cu(NO_3)_2$ solution and then were dried at 110 °C and calcined at 450 °C in N_2 atmosphere. The Cu mass content was measured by inductively coupled plasma (ICP).

The regeneration of the spent catalyst was conducted in a flowing air atmosphere at a rate of 50 mL/min at 580 °C for 5 h. The re-nitridation of the regenerated catalyst was conducted in the same procedure as the nitridation of HBeta zeolites.

Characterizations

Powder XRD (PXRD) patterns were collected on an X-ray diffractometer (Rigaku Smartlab) using Cu Kα radiation (40 kV and 100 mA) with a scanning rate of 8°/min in the range of 2θ = 5°-50°.

N_2 adsorption experiments were performed at -196 °C on Micromeritics ASAP 2460. The samples were pretreated at 300 °C for 4 h before measurements. The total specific surface areas were calculated using the Brunauer-Emmett-Teller (BET) method, and the pore volumes were calculated by N_2 volume adsorbed at relative pressures close to $p/p_0 = 1$.

Nitrogen element analysis was carried out on a Vario EL analyzer with a test temperature of 1,000 °C using oxygen and high-temperature oxidants as additives. Three parallel tests were conducted and the average value was taken.

Ultraviolet-visible (UV-vis) diffuse reflectance spectra were collected from 190-800 nm using a JACSO UV-550 spectrometer.

^{29}Si MAS NMR experiments were conducted on the Agilent DD2-500MHz spectrometer with a resonance frequency at 99.3 MHz using a 6 mm probehead and spinning rate of 6 kHz. The spectra were acquired with a π/4 pulse width of 2.8 μs, a recycle delay of 120 s and 200 scans. Chemical shifts were referenced to tetramethylsilane.

FT-IR experiments were performed on a Thermo Fisher Nicolet iS10 spectrometer equipped with an environmental temperature chamber (PIKE Technologies). All spectra were collected at 25 °C by accumulating 64 scans after the samples were dehydrated at 400 °C for 30 min under flowing N_2 atmosphere. Nicolet OMNIC software converted the absorbance data into Kubelka-Munk format.

CO_2- or NH_3-TPD experiments were performed using a homemade instrument with mass spectrometry (Pfeiffer Omini-star, GSD-320) to characterize the basic and acidic sites over the catalysts, respectively. Typically, 37 mg of sample was used in each measurement. The sample was first purged with nitrogen at 300 °C for 0.5 h at a 10 °C/min heating ramp rate and then cooled down to 100 °C. A flow of 40%vol CO_2/N_2 or 1%vol NH_3/N_2 was introduced into the tubular catalyst bed for 30 min. After purging the catalyst bed for about 2 h with N_2 to remove the physisorbed CO_2 or NH_3, the catalyst was heated up to 750 °C at a 10 °C/min heating ramp rate.

Thermogravimetric (TG) measurements were conducted on an SDT-Q600H TG analyzer at a heating rate of 10 °C/min from room temperature to 800 °C in air flow.

TPO experiments were conducted on a homemade instrument. The samples were raised from 100 to 800 °C at a rate of 10 °C/min in 10% O_2/N_2 gas, and the signal curve of CO_2 in exhaust gas was continuously detected by a mass spectrometer (Pfeiffer Omini-star, GSD-320).

Catalytic test

The formaldehyde conversion with methyl acetate was carried out in a 50 mL stainless steel autoclave. Before reaction, certain amounts of 37% formaldehyde aqueous solution, i.e., formalin, methyl acetate, and catalyst, were added into the reactor. The mixture was stirred at 1,200 ppm with a mechanical stirrer and heated to the desired reaction temperature. After reaction, the liquid products and the solid catalyst were separated by centrifugation, and a certain amount of isopropanol was added as an internal standard. The products were analyzed by a gas chromatograph (Shanghai Tianmei GC-7900) equipped with a flame ionization detector (FID) plus a HP-5 capillary column and a thermal conductivity detector (TCD) plus a packed GDX-403 column. The formaldehyde conversion and selectivity were calculated by:

$$Formaldehyde\ conversion = \frac{m_0 - m}{m_0} \times 100\%$$

$$Selectivity_{MA} = \frac{MA}{MA + \sum m_{by-product}} \times 100\%$$

where m_0 is the mass of formaldehyde fed into the reactor; m is the mass of formaldehyde after reaction; MA and $m_{by\text{-}product}$ stand for the mass of methyl acrylate and by-product derived from formaldehyde, respectively.

The acetone derived from methyl acetate cannot be ignored in the reaction. Therefore, the selectivity of acetone was calculated, based on the consumed methyl acetate, by:

$$Selectivity\ of\ acetone = \frac{n_{acetone}}{n_{MAC}\ consumed} \times 100\%$$

where $n_{acetone}$ and n_{MAC} are the molar quantities of acetone and methyl acetate, respectively.

RESULTS AND DISCUSSION

Aldol condensation catalyzed by NBeta zeolites

As a comparison, the catalytic performance of the aldol condensation over HBeta zeolites was evaluated, and the results are shown in Figure 1. For HBeta, methyl acrylate selectivity is about 82%, and formaldehyde conversion is 90%. Still, lots of by-products were detected over HBeta zeolites. Although the acidic sites were

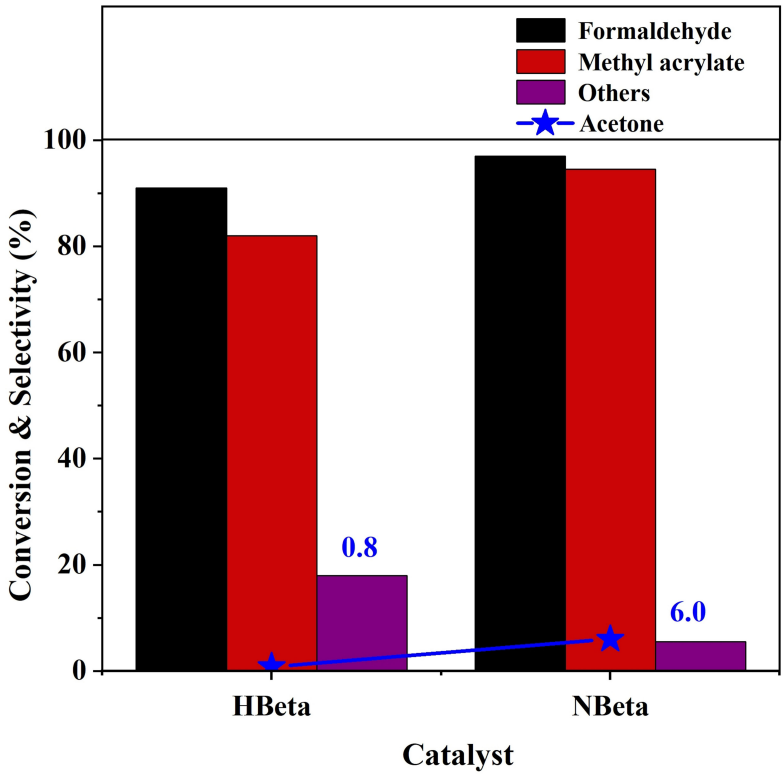

Figure 1. Reaction performance of HBeta zeolites before and after nitridation. Reaction conditions: 320 °C, 6 h, methyl acetate/formaldehyde molar ratio = 4. HBeta: H-form Beta; NBeta: nitrogen-containing Beta.

reported to be essential to improve the aldol condensation[4,14], strong acidic sites lead to many side reactions such as olefin polymerization and cracking to increase by-product and coke contents. After nitridation, formaldehyde conversion and methyl acrylate selectivity increase to 97% and 94%, respectively, over NBeta catalyst. This indicates that nitridation can enhance the catalytic performance of aldol condensation. We also calculated the acetone selectivity in the by-products based on methyl acetate. It is 6% on NBeta zeolites, higher than HBeta zeolites. This demonstrates that although the increase of basic sites after nitridation improves the methyl acrylate selectivity, it will also form acetone due to the self-condensation of methyl acetate[32,33]. That is to say, both the acidity and basicity of the catalyst significantly influence the reaction performance. The nitridation conditions could affect the acidity and basicity balance of the catalyst. Therefore, we evaluated and optimized the reaction performance of NBeta zeolites prepared under different nitridation conditions, and the results are shown in Supplementary Figures 1-3. By adjusting the nitridation temperature and time and NH_3 flow rate, it was found that NB-800 catalyst exhibited the best performance in the aldol condensation after nitridation in 65 mL/min NH_3 at 800 °C for 12 h. A formaldehyde conversion of 97% and methyl acetate selectivity of 94% was achieved on NB-800 catalyst; therefore, it was selected as a potential catalyst for optimizing aldol reaction conditions.

Effect of the aldol reaction conditions

The effect of reaction temperature in the range of 300-360 °C on the aldol reaction performance was investigated over NB-800 catalyst and the results are shown in Figure 2. It can be seen that the reaction temperature greatly influences the selectivity of methyl acrylate. When the reaction temperature rises from 300 to 320 °C, the selectivity of methyl acrylate increases from 70% to 94% and that of others decreases from 23% to 3%. When the reaction temperature exceeds 320 °C, the selectivity of by-products increases,

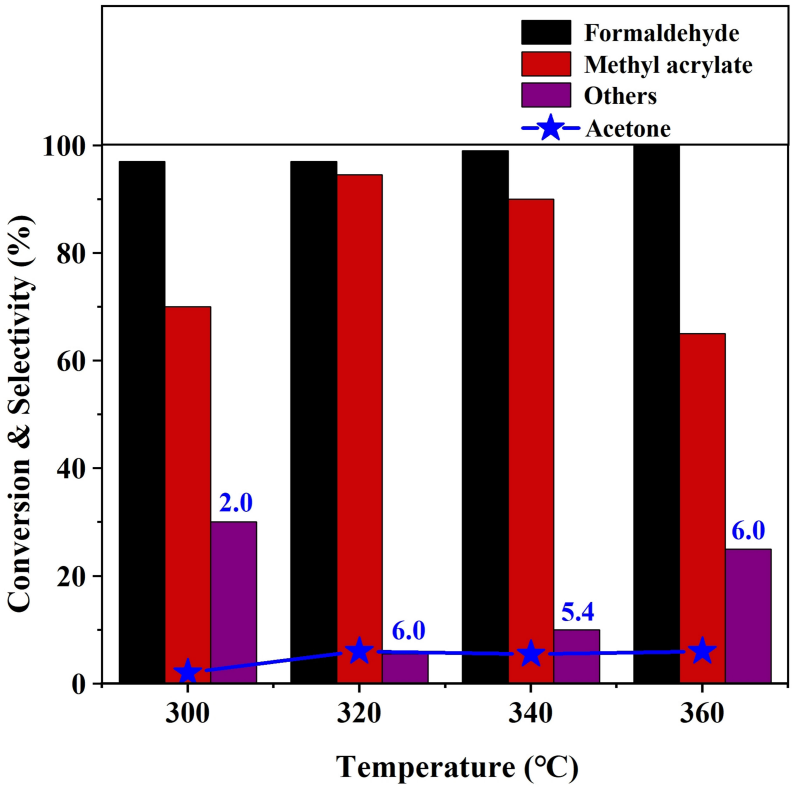

Figure 2. Effect of reaction temperature on catalytic performance of aldol condensation. Reaction conditions: 0.1 g NB-800, 6 h, methyl acetate/formaldehyde molar ratio = 4.

decreasing methyl acrylate selectivity. The conversion of formaldehyde is close to 100% without significant change upon reaction temperature. Given both the conversion and selectivity, the optimal reaction temperature is 320 °C. We also optimized other reaction conditions on the NB-800 catalyst for the aldol condensation [Supplementary Figures 4-6]. A formaldehyde conversion of 97% and methyl acrylate selectivity of 94% were achieved at optimal 320 °C, reaction time of 6 h, methyl acetate/formaldehyde molar ratio of 4, and catalyst mass of 0.1 g.

Effect of the acidity and basicity on the catalytic performance

It can be seen from Figure 1 that after nitridation of HBeta zeolites, both the formaldehyde conversion and the methyl acrylate selectivity are enhanced, but the acetone selectivity, a by-product produced by the self-condensation of methyl acetate, also increases. Basically, the production of by-product acetone may be due to the strong basicity of the catalyst[32,33]. In general, copper oxide is used as a mild Lewis acid site in many reactions[34]. Thus, Cu was loaded on NBeta catalyst in order to tune the acid-base balance and further improve the reaction performance. As shown in Figure 3, as Cu content increases from 1% to 4%, the acetone selectivity decreases from 6% to ~1%, and the formaldehyde conversion is nearly unchanged. However, too much Cu addition decreases the methyl acrylate selectivity. Overall, 2 wt% Cu/NB-800 exhibits the best methyl acrylate selectivity of 95%, formaldehyde conversion of 99%, and the acetone selectivity is only 1.3%. In this case, the carbon balance was calculated to be 91%. We also compared the reaction performance of 2 wt% Cu/NB-800 and 2 wt% Cu/HBeta catalysts in Supplementary Figure 7. It is found that 2 wt% Cu/NB-800 shows both higher formaldehyde conversion and methyl acrylate selectivity than 2 wt% Cu/HBeta. This further indicates that a proper balance of acidity and basicity on NBeta zeolites benefits the aldol condensation.

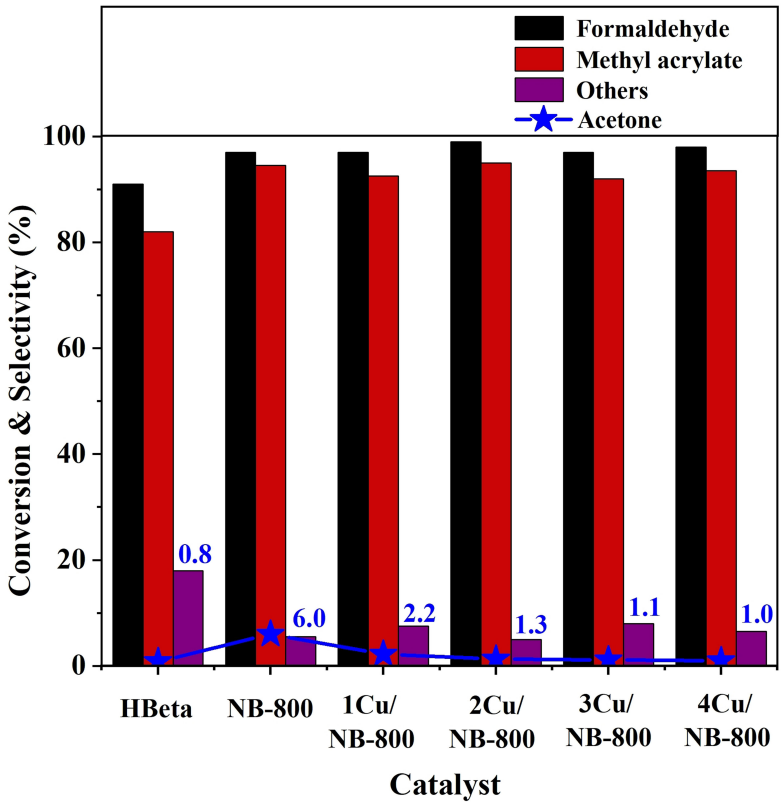

Figure 3. Effect of Cu loading on catalytic performance of aldol condensation. Reaction conditions: 320 °C, 6 h, methyl acetate/formaldehyde molar ratio = 4. HBeta: H-form Beta; NBeta: nitrogen-containing Beta.

Catalyst characterization

XRD, N_2 adsorption and nitrogen elemental analysis

Figure 4 shows the XRD patterns of HBeta and NB-800 zeolites with different Cu contents. It can be seen that all samples have the typical Beta zeolite structure[35]. After nitridation and loading Cu, the positions of the main diffraction peaks of the zeolites remain unchanged, and there is no diffraction peak of CuO due to its high dispersion on the surface of zeolites[36]. Nevertheless, the intensities of the diffraction peaks slightly decrease. This is possibly due to the reduced crystallinity caused by the partial collapse of the framework during nitridation at a temperature as high as 800 °C. Introducing a small amount of Cu does not alter the framework structure of NBeta zeolites while more Cu added causes the partial loss of crystallinity probably due to the stronger interaction between Cu acting as acid sites and basic sites on NBeta zeolites. The textural properties of the samples were determined by N_2 adsorption-desorption isotherms in Supplementary Figure 8. The specific BET surface areas, pore volumes and nitrogen contents of HBeta and Cu/NBeta zeolites are summarized in Table 1. After nitridation, the specific surface area and pore volume of HBeta decrease obviously, but NBeta still possesses large surface area and pore volume and its nitrogen content is up to 2.1 wt%. The addition of 1 wt% - 3 wt% Cu gradually decreases the surface area and the pore volume, but 4 wt% Cu causes a remarkable reduction in the surface area and the pore volume. UV-vis spectra of Cu/NBeta zeolites are demonstrated in Supplementary Figure 9. It shows that most of the Cu species exist in the form of isolated Cu^{2+}. When the Cu loading increases to 4 wt%, the number of clustered CuO species increases readily. This may be the reason for the sharp decrease in the surface area and pore volume. There is no significant change in the nitrogen content of the samples modified by Cu [Table 1].

Table 1. BET surface areas, pore volumes and N contents of the samples studied herein

Samples	S_{BET} (m^2/g)	V_{pore} (cm^3/g)	N content (wt%)
HBeta	568	0.29	-
NB-800	436	0.26	2.1
1Cu/NB-800	385	0.22	1.9
2Cu/NB-800	373	0.22	2.0
3Cu/NB-800	367	0.21	1.7
4Cu/NB-800	334	0.19	2.0

BET: Brunauer-Emmett-Teller; HBeta: H-form Beta.

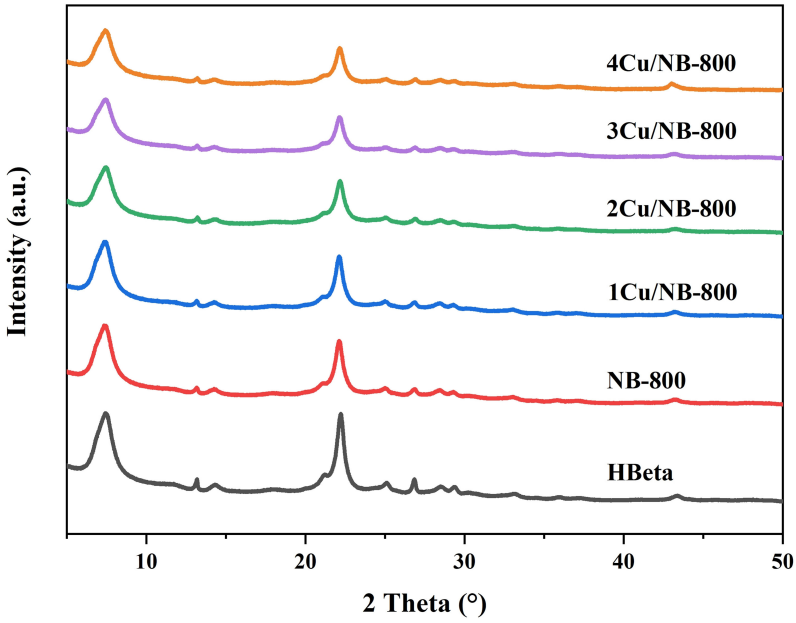

Figure 4. XRD patterns of HBeta and NBeta zeolites with different Cu loadings. XRD: X-ray diffraction; HBeta: H-form Beta; NBeta: nitrogen-containing Beta.

^{29}Si MAS NMR and FT-IR spectra

The formation of different NH_x species on the surface of nitrogen-containing samples can be detected by ^{29}Si MAS NMR and FT-IR spectroscopy. Figure 5A presents the ^{29}Si MAS NMR spectra of HBeta and NBeta with different Cu contents. The signals at around -112 and -116 ppm can be assigned to $Si(OSi)_4$ species in Beta zeolites. The signal at -107 ppm belongs to $Si(OAl)(OSi)_3$ species. Additionally, the signal at -103 ppm is attributed to $Si(OH)(OSi)_3$ groupings[37,38]. After nitridation, a new resonance peak appears at -93 ppm in NBeta zeolites, which is attributed to Si–N bonds[39]. This indicates that N atoms have substituted partial O atoms to enter the framework of Beta zeolites. The addition of Cu did not lead to the disappearance of such Si-N species, which is consistent with the results of nitrogen element analysis.

Figure 5B shows the FT-IR spectra of HBeta and NBeta with different Cu loadings. The spectrum of the parent HBeta zeolites shows bands at ~3,743 and 3,607 cm^{-1}, which are assigned to silanols and bridging Si-OH-Al hydroxyls, respectively[29]. After nitridation at 800 °C, the two peaks mentioned above are sharply decreased, and the new bands at *ca.* 3,417, 3,395 and 3,339 cm^{-1} appear, which are sequentially assigned to $Si-NH_2$, Si-NH-Si and $Si-NH_2$-Al moieties[40,41]. This demonstrates that during the nitridation process, NH_3

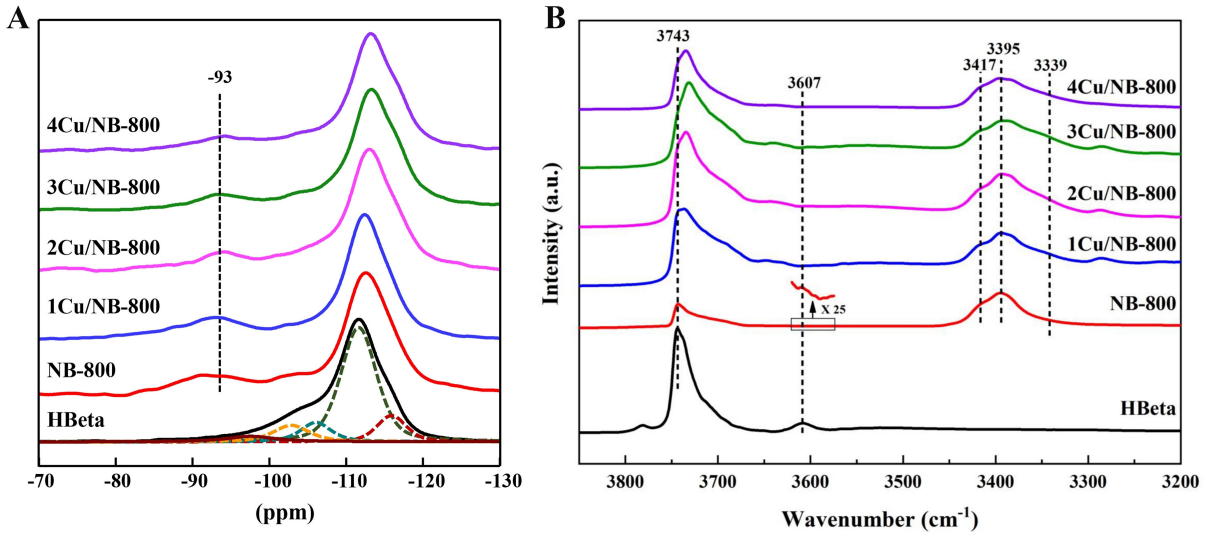

Figure 5. (A) ^{29}Si MAS NMR and (B) FT-IR spectra of HBeta and NBeta zeolites with different Cu loadings. ^{29}Si MAS NMR: Silicon-29 magic angle spinning nuclear magnetic resonance; FT-IR: Fourier transform infrared spectroscopy; HBeta: H-form Beta; NBeta: nitrogen-containing Beta.

reacts with Si-OH and Si-OH-Al to form Si-NH_2 and Si-NH_2-Al, respectively. Besides, part of Si-NH_2 continues to react with Si-OH or Si-NH_2 to form Si-NH-Si[40]. This also proves that N atoms replace part of O atoms in the framework of Beta zeolites, which is consistent with the results from ^{29}Si MAS NMR and nitrogen element analysis. After the modification of NBeta with Cu, the bands at ~3,417, 3,395 and 3,339 cm^{-1} still exist, indicating almost no loss of N atoms during the loading of Cu. In addition, the peaks associated with extra-framework AlOH species increase at 3,733 and 3,691 cm^{-1} for NBeta loaded with Cu, possibly due to the dissociation of hydrolyzed $[Al(OH)_2]^+$ cations promoted by copper ions[42].

NH_3-TPD and CO_2-TPD profiles

The acidity of HBeta and NBeta with different Cu loadings was investigated using the NH_3-TPD technique [Figure 6A]. The number of different acidic sites can be quantitatively calculated from the deconvoluted signal areas under the corresponding TPD curve[43], and the results are listed in Table 2. Apparently, both the nitridation and the modification of Cu have a certain impact on the amount and strength of the acidic sites over Beta zeolites. According to the peak fitting of the spectrum, HBeta zeolites have three obvious NH_3 desorption peaks centered at 230, 340 and 500 °C, which belong to the weak, medium-strength and strong acidic sites, respectively. The strong and medium-strength acidic sites of NBeta disappear with only a small amount of weak acidic sites left [Table 2], indicating the nitridation decreases both the amount and the strength of the acidic sites over HBeta, which may be due to the substitution of O atoms by N atoms after high-temperature nitridation[44]. After the modification of NBeta with Cu, the number of acidic sites, especially the medium-strength and strong acidic sites, increases with rising Cu content from 1 wt% to 4 wt%. Furthermore, 1Cu/NB-800 has more medium-strength acidic sites than NB-800. When Cu loading increases to 2 wt%, strong acidic sites appear with an NH_3 desorption signal at 410 °C, whose acid strength is lower than HBeta. The number of medium-strength and strong acidic sites gradually increases as Cu content rises from 2 wt% to 4 wt%. However, the total acid amount is far lower than that of HBeta.

Figure 6B shows the basicity characterization results from CO_2-TPD measurement. The number of basic sites of corresponding samples is listed in Table 2. HBeta zeolites have only one CO_2 desorption peak centered at 380 °C, indicating HBeta zeolites have a few weak basic sites[45]. After nitridation, new CO_2

Table 2. Acidic and basic properties of HBeta and Cu/NBeta catalysts with different Cu contents

Samples	Acidic site (μmol/g)			Total acid amount (μmol/g)	Basic site (μmol/g)			Total base amount (μmol/g)
	Weak	Middle	Strong		Weak	Middle	Strong	
HBeta	12	71	47	130	1.9	-	-	1.9
NB-800	3	-	-	3	1.1	8.0	2.1	11.2
1Cu/NB-800	4	5	-	9	2.0	5.8	1.8	9.6
2Cu/NB-800	3	10	3	16	2.3	5.0	-	7.3
3Cu/NB-800	5	15	8	28	0.4	2.0	-	2.4
4Cu/NB-800	5	15	13	33	0.4	1.7	-	2.1

HBeta: H-form Beta; NBeta: nitrogen-containing Beta.

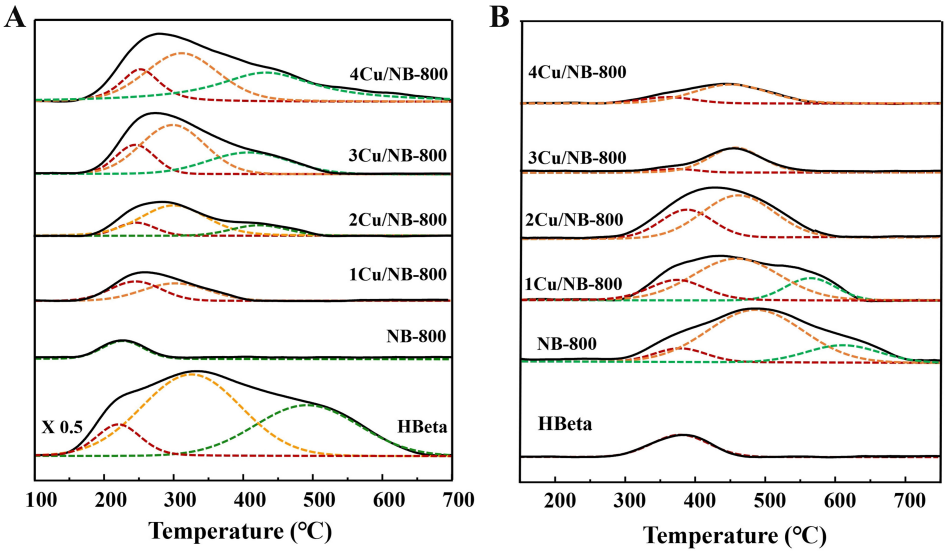

Figure 6. (A) NH_3-TPD and (B) CO_2-TPD profiles of HBeta and NBeta zeolites with different Cu loadings. TPD: Temperature-programmed desorption; HBeta: H-form Beta; NBeta: nitrogen-containing Beta.

desorption peaks centered at ~480 and ~610 °C appear, which are attributed to the medium-strength and strong basic sites. Both the amount and the strength of basic sites over NBeta increase obviously compared to HBeta. After addition of Cu, both the amount and the strength of basic sites over NBeta decrease. The strong basic sites disappear when Cu content increases to 2 wt% and the number of basic sites decreases gradually with the Cu content. This indicates that the addition of Cu mainly covers the strong basic sites, and excessive Cu addition also has a certain impact on the medium-strength basic sites.

By correlating the characterization results of NH_3- and CO_2-TPD with the reaction performance, we can conclude that both the acidity and basicity influence the catalytic performance. HBeta gives lower selectivity to methyl acrylate due to large amounts of other products formed over strong acidic sites. Nitridation of Beta decreases the acidic sites and increases the basic sites. Thus, NBeta shows higher selectivity to methyl acrylate than HBeta, which means that decreased acidic sites and increased basic sites could inhibit the side reactions and boost the aldol reaction. However, NBeta displays higher selectivity to acetone than HBeta, indicating that although the basic sites can boost the aldol reaction, strong basic sites are unfavorable for the whole reaction due to the formation of acetone. Adding Cu decreases both the amount and the strength of the basic sites over NBeta and thus inhibits the formation of acetone. In addition, the increase of medium-

strength acidic sites with an appropriate amount after the addition of Cu is also beneficial for the aldol reaction, i.e., the activation of formaldehyde and the dehydration of the intermediate aldol to methyl acrylate. However, the selectivity to others increases over 4Cu/NBeta due to the presence of strong acidic sites. Furthermore, 2Cu/NBeta with a proper number of basic sites and acidic sites with medium strength results in *ca.* 95% methyl acrylate selectivity and only about 1% acetone selectivity.

TG/DTG analysis

The TG analysis results of different samples after reaction are shown in Figure 7. TG profiles in Figure 7A display two obvious weight loss peaks centered at ~380 and ~535 °C according to the derivative thermogravimetry (DTG) results in Figure 7B. Combined with the TPO measurement shown in Supplementary Figure 10, no CO_2 signal is found when the temperature is lower than 200 °C, indicating that the weight-loss peak before 200 °C in Figure 7B is from water on the catalyst surface. Based on DTG and TG diagrams, the main carbon weight-loss peak on HBeta appears at about 535 °C with only a weak weight-loss peak at ~380 °C. This can be attributed to the carbon deposits formed on the strong acidic centers and weak acidic centers of the catalyst[9], respectively. For spent HBeta, the coke content reaches as high as ~28%. For NBeta after aldol reaction, the coke content decreases to 20% owing to the reduced acid strength and density on Beta zeolites. When Cu was introduced on NBeta, the coke content further decreases to ~17%. This means that a balanced acidity and basicity on 2Cu/NBeta enhanced the aldol reaction performance and reduced the by-products that may cause coke.

Successive regeneration of spent Cu/NBeta catalyst

The regeneration capability of spent catalyst is very important for its practical applications. Figure 8 shows that both formaldehyde conversion and methyl acrylate selectivity can be properly restored after three successive regeneration cycles of the 2 wt% Cu/NBeta catalyst. Formaldehyde conversion decreases from *ca.* 99% to 86%, and methyl acrylate selectivity decreases slightly from 95% to 90% after the fourth regeneration cycle.

The 2 wt% Cu/NBeta catalyst before and after regeneration was characterized by XRD, ^{29}Si MAS NMR, and CO_2-TPD to investigate the deactivation mechanism during regeneration by air. XRD patterns of the catalyst before and after regeneration in Supplementary Figure 11 indicate the intensities of the characteristic diffraction peaks decrease gradually after successive regeneration cycles. The intensity of the diffraction peak at 35.6° rises with the increase of the cycling numbers. This may be due to the accumulation of some unremoved coke on one of the crystal faces as the cycling numbers increase. ^{29}Si MAS NMR was employed to characterize the local structures of the catalyst before and after regeneration [Figure 9]. The Si-N signal at -93 ppm can be restored to some extent after regeneration, ensuring the high selectivity to methyl acrylate. However, the Si-N species decrease gradually with the increase of regeneration times. After the fourth regeneration, the Si-N signal basically disappears. We further investigated the basicity of 2Cu/NBeta before and after regeneration by CO_2-TPD [Figure 9], and the quantity of basic sites is provided in Supplementary Table 1. The total number of basic sites decreases gradually from 7.3 to 2.1 μmol/g after four successive regenerations, which is consistent with the results from ^{29}Si MAS NMR. Meanwhile, the total amounts of acidic sites increase from 16 to 21.4 μmol/g determined by NH_3-TPD [Figure 9 and Supplementary Table 1], indicating that the increase of cycling times results in the decrease of basic sites and increase of acidic sites of the catalyst. This may lead to the decrease of selectivity to methyl acrylate. We speculate that this phenomenon may be caused by the replacement of N atoms by O atoms during the successive regenerations in air. If so, the regenerated catalyst was re-nitridated in ammonia, and the Si–N bonds may be recovered. Indeed [Figure 9A], the Si-N signal at -93 ppm appears again on the re-nitridated RE-5-N sample. And the total basic sites and acidic sites on this sample are almost restored to those of the fresh 2Cu/NBeta catalyst. Additionally, the intensity of the diffraction peak at 35.6° decreases remarkably in

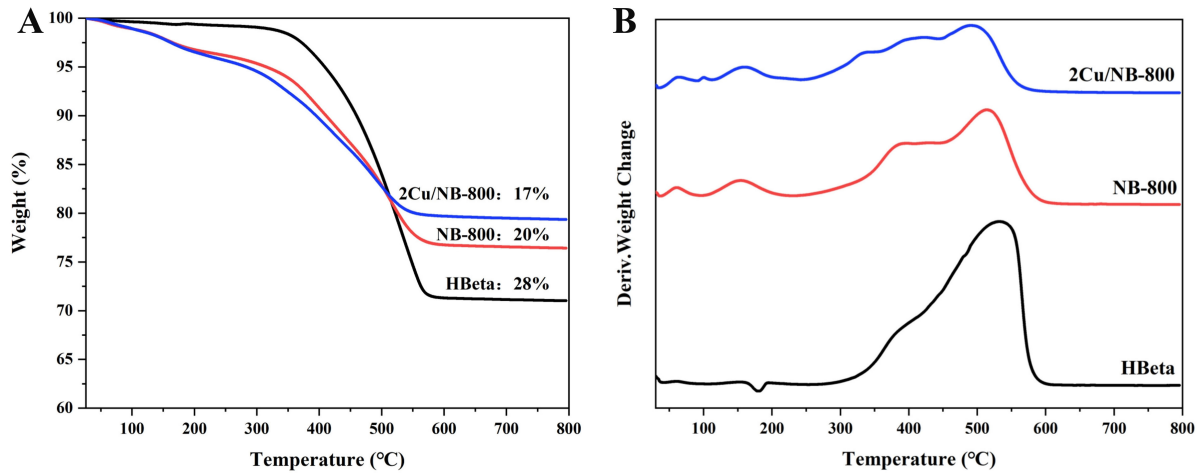

Figure 7. (A) TG and (B) DTG profiles of spent HBeta and Cu/NBeta catalysts. TG: Thermogravimetry; DTG: derivative thermogravimetry; HBeta: H-form Beta.

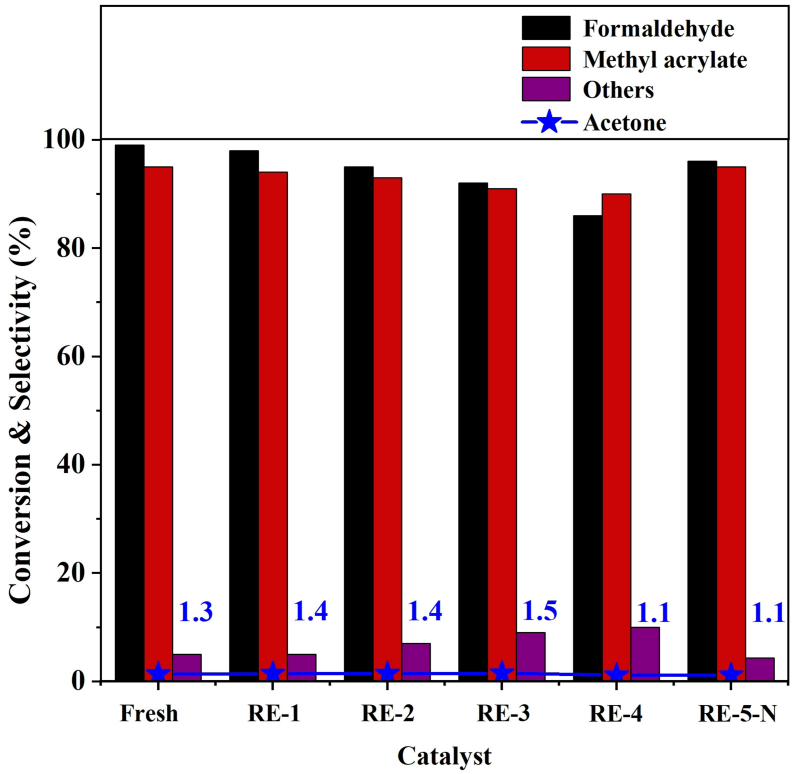

Figure 8. Catalytic performance of spent 2Cu/NBeta after successive regeneration cycles. NBeta: Nitrogen-containing Beta.

the XRD pattern of the RE-5-N sample. This means the coke that cannot be completely removed during the regeneration process was further eliminated in the re-nitridation process at higher temperatures. All these factors result in the recovery of the catalytic performance of the RE-5-N sample to that of the fresh catalyst [Figure 8].

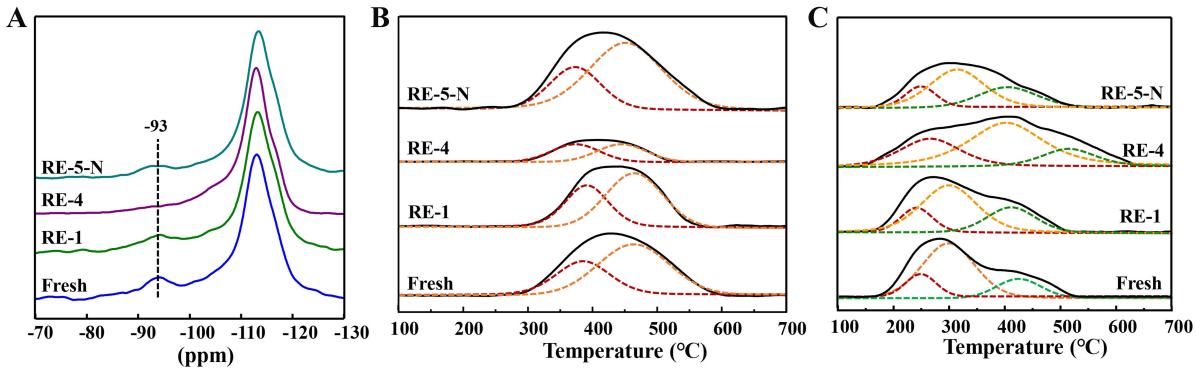

Figure 9. (A) ^{29}Si MAS NMR spectra, (B) CO_2-TPD and (C) NH_3-TPD profiles of the 2Cu/NBeta before and after regeneration cycles. ^{29}Si MAS NMR: Silicon-29 magic angle spinning nuclear magnetic resonance; TPD: temperature-programmed desorption; NBeta: Nitrogen-containing Beta.

CONCLUSIONS

In this study, the catalytic performance of the one-step condensation of bio-based formaldehyde and methyl acetate to renewable methyl acrylate was evaluated over Cu-modified NBeta catalysts. ^{29}Si MAS NMR, FT-IR, NH_3-TPD, CO_2-TPD, and nitrogen element analysis reveal that nitridation reduces the strength and quantity of acidic sites and increases the basic sites because of the Si–N bond formation in the framework of Beta zeolites. This benefits promoting the methyl acrylate selectivity and reducing the coke content. However, strong basic sites over NBeta zeolites result in the by-product acetone. The modification of Cu decreases the strong basic sites of NBeta and introduces moderate acid sites, thus inhibiting the formation of acetone. High methyl acrylate selectivity of 95% and formaldehyde conversion of 99% were achieved over Cu/NBeta acid-base bifunctional catalyst with proper medium-strength acidic and basic sites in optimized conditions. The coke content of the spent catalyst is lowered from 28% on HBeta to 17% on Cu/NBeta. It has a certain regeneration capability. After four times of regeneration cycles, the reaction performance decreases slightly due to the weakening of the Si-N species. However, the re-nitridation of the regenerated catalyst results in the recovery of the catalytic performance.

DECLARATIONS

Authors' contributions

Carried out experiments, analyzed data, interpreted results, and wrote the draft manuscript: Wang M
Analyzed data and discussed results: Xu L
Directed and supervised the project, discussed results, and revised the manuscript: Zhang W

Availability of data and materials

The data supporting this article have been included as part of the Supplementary Materials.

Financial support and sponsorship

The financial support from the National Natural Science Foundation of China (No. 21673027) was acknowledged.

Conflicts of interest

All authors declared that there are no conflicts of interest.

Ethical approval and consent to participate

Not applicable.

Consent for publication

Not applicable.

Copyright

REFERENCES

1. Wang G, Li Z, Li C, Zhang S. Preparation of methyl acrylate from methyl acetate and methanol with mild catalysis of cobalt complex. *Chem Eng J* 2019;359:863-73. DOI
2. Xu A, Wang Y, Ge H, Chen S, Li Y, Lu W. An outstanding Cr-doped catalyst for selective oxidation of propane to acrylic acid. *Chin J Catal* 2013;34:2183-91. DOI
3. Fang W, Ge Q, Yu J, Xu H. Catalytic selective oxidation of propane to acrylic acid in a fixed-bed reactor with an O_2-distributor. *Ind Eng Chem Res* 2011;50:1962-7. DOI
4. Xie M, Ni Y, Fang X, et al. Nano-sized H-ZSM-5 zeolite catalyzes aldol condensation reaction to prepare methyl acrylate and acrylic acid. *Catal Sci Technol* 2022;12:5171-7. DOI
5. He T, Qu Y, Wang J. Aldol condensation reaction of methyl acetate and formaldehyde over cesium oxide supported on silica gel: an experimental and theoretical study. *Catal Lett* 2019;149:373-89. DOI
6. Ma Z, Ma X, Liu H, Zhu W, Guo X, Liu Z. One-step aldol condensation reaction of dimethoxymethane and methyl acetate over supported Cs/ZSM-35 zeolite catalysts. *Chin J Catal* 2018;39:1129-37. DOI
7. Gautam P, Neha, Upadhyay S, Dubey S. Bio-methanol as a renewable fuel from waste biomass: current trends and future perspective. *Fuel* 2020;273:117783. DOI
8. Khalameida S, Nebesnyi R, Pikh Z, et al. Catalytic aldol condensation of formaldehyde with acetic acid on titanium phosphates modified by different techniques. *Reac Kinet Mech Cat* 2018;125:807-25. DOI
9. Ma Z, Ma X, Ni Y, et al. HZSM-35 zeolite catalyzed aldol condensation reaction to prepare acrylic acid and its ester: effect of its acidic property. *Chin J Catal* 2018;39:1762-9. DOI
10. Li J, Tai J, Davis RJ. Hydrocarbon oxidation and aldol condensation over basic zeolite catalysts. *Catal Today* 2006;116:226-33. DOI
11. Bao Q, Bu T, Yan J, et al. Synthesis of methyl acrylate by aldol condensation of methyl acetate with formaldehyde over Al_2O_3-supported barium catalyst. *Catal Lett* 2017;147:1540-50. DOI
12. Zhang G, Zhang H, Yang D, Li C, Peng Z, Zhang S. Catalysts, kinetics and process optimization for the synthesis of methyl acrylate over Cs-P/γ-Al_2O_3. *Catal Sci Technol* 2016;6:6417-30. DOI
13. Yang D, Li D, Yao H, et al. Reaction of formalin with acetic acid over vanadium-phosphorus oxide bifunctional catalyst. *Ind Eng Chem Res* 2015;54:6865-73. DOI
14. Dumitriu E, Hulea V, Fechete I, Auroux A, Lacaze J, Guimon C. The aldol condensation of lower aldehydes over MFI zeolites with different acidic properties. *Microporous Mesoporous Materials* 2001;43:341-59. DOI
15. Wang Y, Chen H, Zhao G, Liu M, Lang X, Zhu Z. Influence of support properties on the activity of basic catalysts for aldol condensation of formaldehyde and methyl acetate in a continuous-flow reactor. *J Flow Chem* 2015;5:87-94. DOI
16. He T, Qu Y, Wang J. Experimental and theoretical study for vapor phase aldol condensation of methyl acetate and formaldehyde over alkali metal oxides supported on SBA-15. *Ind Eng Chem Res* 2018;57:2773-86. DOI
17. Yan J, Zhang C, Ning C, et al. Vapor phase condensation of methyl acetate with formaldehyde to preparing methyl acrylate over cesium supported SBA-15 catalyst. *J Ind Eng Chem* 2015;25:344-51. DOI
18. Zeidan R, Davis M. The effect of acid-base pairing on catalysis: an efficient acid-base functionalized catalyst for aldol condensation. *J Catal* 2007;247:379-82. DOI
19. Tichit D, Lutic D, Coq B, Durand R, Teissier R. The aldol condensation of acetaldehyde and heptanal on hydrotalcite-type catalysts. *J Catal* 2003;219:167-75. DOI
20. Bao Q, Zhu W, Yan J, et al. Vapor phase aldol condensation of methyl acetate with formaldehyde over a Ba-La/Al_2O_3 catalyst: the stabilizing role of La and effect of acid-base properties. *RSC Adv* 2017;7:52304-11. DOI
21. Guo X, Yang D, Zuo C, Peng Z, Li C, Zhang S. Catalysts, process optimization, and kinetics for the production of methyl acrylate over vanadium phosphorus oxide catalysts. *Ind Eng Chem Res* 2017;56:5860-71. DOI
22. Zhao H, Zuo C, Yang D, Li C, Zhang S. Effects of support for vanadium phosphorus oxide catalysts on vapor-phase aldol condensation of methyl acetate with formaldehyde. *Ind Eng Chem Res* 2016;55:12693-702. DOI
23. Hu J, Lu Z, Yin H, et al. Aldol condensation of acetic acid with formaldehyde to acrylic acid over SiO_2-, SBA-15-, and HZSM-5-supported V-P-O catalysts. *J Ind Eng Chem* 2016;40:145-51. DOI
24. Yang D, Sararuk C, Suzuki K, Li Z, Li C. Effect of calcination temperature on the catalytic activity of VPO for aldol condensation of acetic acid and formalin. *Chem Eng J* 2016;300:160-8. DOI

25. Feng X, Sun B, Yao Y, Su Q, Ji W, Au C. Renewable production of acrylic acid and its derivative: New insights into the aldol condensation route over the vanadium phosphorus oxides. *J Catal* 2014;314:132-41. DOI
26. Zhang C, Xu Z, Wan K, Liu Q. Synthesis, characterization and catalytic properties of nitrogen-incorporated ZSM-5 molecular sieves with bimodal pores. *Appl Catal A Gen* 2004;258:55-61. DOI
27. Lesthaeghe D, Van Speybroeck V, Marin GB, Waroquier M. DFT investigation of alkoxide vs alkylammonium formation in amine-substituted zeolites. *J Phys Chem B* 2005;109:7952-60. DOI PubMed
28. Kweon S, An H, Shin C, Park MB, Min H. Nitrided Ni/N-zeolites as efficient catalysts for the dry reforming of methane. *J CO2 Util* 2021;46:101478. DOI
29. Lyu J, Hu H, Rui J, et al. Nitridation: A simple way to improve the catalytic performance of hierarchical porous ZSM-5 in benzene alkylation with methanol. *Chin Chem Lett* 2017;28:482-6. DOI
30. Wang T, Wu G, Guan N, Li L. Nitridation of MgO-loaded MCM-41 and its beneficial applications in base-catalyzed reactions. *Microporous Mesoporous Mater* 2012;148:184-90. DOI
31. Liu Y, Xu L, Zhang W. Formaldehyde and isobutene condensation via Prins reaction on HY zeolites treated with NH_3. *Fine Chem* 2020;37:2069-75. (in Chinese) Available from: https://link.cnki.net/doi/10.13550/j.jxhg.20200332. [Last accessed on 16 Apr 2024]
32. Boekaerts B, Sels BF. Catalytic advancements in carboxylic acid ketonization and its perspectives on biomass valorisation. *Appl Catal B Environ* 2021;283:119607. DOI
33. Mekhemer GAH, Halawy SA, Mohamed MA, Zaki MI. Ketonization of acetic acid vapour over polycrystalline magnesia: in situ Fourier transform infrared spectroscopy and kinetic studies. *J Catal* 2005;230:109-22. DOI
34. Xu L, Liu S, Meng X, et al. A novel tandem route to renewable isoprene over Mo-Fe oxide and mesoporous Cu/MgO composite catalysts. *Appl Catal B Environ* 2024;341:123341. DOI
35. Xu L, Zhao R, Zhang W. One-step high-yield production of renewable propene from bioethanol over composite $ZnCeO_x$ oxide and HBeta zeolite with balanced Brönsted/Lewis acidity. *Appl Catal B Environ* 2020;279:119389. DOI
36. Sagar GV, Rao PV, Srikanth CS, Chary KV. Dispersion and reactivity of copper catalysts supported on Al_2O_3-ZrO_2. *J Phys Chem B* 2006;110:13881-8. DOI PubMed
37. He LH, Li JJ, Han SY, et al. Dynamic evolution of HZSM-5 zeolite framework under steam treatment. *Chem Synth* 2024;4:1. DOI
38. Zhao R, Xu L, Huang S, Zhang W. Highly selective production of renewable *p*-xylene from bio-based 2,5-dimethylfuran and ethylene over Al-modified H-Beta zeolites. *Catal Sci Technol* 2019;9:5676-85. DOI
39. Dogan F, Hammond KD, Tompsett GA, et al. Searching for microporous, strongly basic catalysts: experimental and calculated ^{29}Si NMR spectra of heavily nitrogen-doped Y zeolites. *J Am Chem Soc* 2009;131:11062-79. DOI PubMed
40. Narasimharao K, Hartmann M, Thiel HH, Ernst S. Novel solid basic catalysts by nitridation of zeolite beta at low temperature. *Microporous Mesoporous Mater* 2006;90:377-83. DOI
41. Kawano A, Moteki T, Ogura M. Effect of delamination on active base site formation over nitrided MWW-type zeolite for Knoevenagel condensation. *Microporous Mesoporous Mater* 2020;299:110104. DOI
42. Shutilov RA, Zenkovets GA, Paukshtis EA, Gavrilov VY. Localization of the copper-containing component in the pore volume of zeolite ZSM-5. *Kinet Catal* 2014;55:243-51. DOI
43. Khallouk K, Solhy A, Idrissi N, Flaud V, Kherbeche A, Barakat A. Microwave-assisted selective oxidation of sugars to carboxylic acids derivatives in water over zinc-vanadium mixed oxide. *Chem Eng J* 2020;385:123914. DOI
44. Wu G, Guan N, Li L. Recent development of nitrogen-incorporated molecular sieves. *Chin J Catal* 2012;33:51-9. (in Chinese) Available from: https://guan.nankai.edu.cn/_upload/article/files/36/25/0754df344c98aa75e4d1d1632b97/da5cafcc-5073-4f51-82ad-74c148c43938.pdf. [Last accessed on 16 Apr 2024]
45. Barthomeuf D. Framework induced basicity in zeolites. *Microporous Mesoporous Mater* 2003;66:1-14. DOI